Neuron
Review

Soft Materials in Neuroengineering for Hard Problems in Neuroscience

Jae-Woong Jeong,[1,3] Gunchul Shin,[1] Sung Il Park,[1] Ki Jun Yu,[2] Lizhi Xu,[1] and John A. Rogers[1,2,*]
[1]Department of Materials Science and Engineering, Frederick Seitz Materials Research Laboratory, University of Illinois at Urbana-Champaign, Urbana, IL 61801, USA
[2]Department of Electrical and Computer Engineering, Frederick Seitz Materials Research Laboratory, University of Illinois at Urbana-Champaign, Urbana, IL 61801, USA
[3]Present address: Department of Electrical, Computer, and Energy Engineering, University of Colorado, Boulder, CO 80309, USA
*Correspondence: jrogers@illinois.edu
http://dx.doi.org/10.1016/j.neuron.2014.12.035

We describe recent advances in soft electronic interface technologies for neuroscience research. Here, low modulus materials and/or compliant mechanical structures enable modes of soft, conformal integration and minimally invasive operation that would be difficult or impossible to achieve using conventional approaches. We begin by summarizing progress in electrodes and associated electronics for signal amplification and multiplexed readout. Examples in large-area, surface conformal electrode arrays and flexible, multifunctional depth-penetrating probes illustrate the power of these concepts. A concluding section highlights areas of opportunity in the further development and application of these technologies.

Introduction

Breakthroughs in fundamental science often follow from advances in technology and methodology. In neuroscience, development of functional magnetic resonance imaging (fMRI) led to key insights into the patterns of activity that occur across the entire brain (Logothetis, 2008). Confocal microscopy and two-photon techniques with genetically encoded fluorescent indicators of membrane voltage, ion concentrations, and synaptic transmission, yielded similar advances in understanding through real-time monitoring of neuronal activity with improved spatial and temporal resolution (Denk and Svoboda, 1997; Fine et al., 1988). Positron emission tomography provided molecular level neuroimaging capabilities for diagnosing brain disorders such as Alzheimer's disease (Phelps, 2000). The emergence of optogenetic techniques (Deisseroth, 2011), methods for rendering brain tissue optically transparent (Chung et al., 2013), miniaturized fluorescence microscopes for cellular-level brain imaging in freely moving animals (Flusberg et al., 2008; Ghosh et al., 2011), and transgenic multicolor labeling strategies for neurons (Livet et al., 2007) represent some of the latest examples in which new technical approaches are enabling fundamental discoveries.

Recently launched, large-scale research initiatives seek to build on these and other technologies to revolutionize our understanding of the human brain. An ambitious goal is to develop neural interface systems that can reveal the interactions of individual cells and entire neural circuits in both time and space. Although optical and chemical techniques can play important roles, capabilities for electrical measurement and stimulation are essential not only to this type of fundamental research in neuroscience, but also to the development of procedures for treating Alzheimer's disease, Parkinson's disease, epilepsy, depression, and many other conditions that originate from aberrant neural behavior. Modern electrical neural interface systems build on a long history, largely involving the development of advanced electrode technologies. Penetrating pins formed in micromachined silicon represent popular means for interfacing directly to brain tissue (Campbell et al., 1991; HajjHassan et al., 2008), whereas bulk metal electrodes and coupling gels provide for measurement through the skin of the scalp (Niedermayer and Lopes Da Silva, 2005). Although effective for many purposes, such systems rely on hard materials in geometrical forms that establish a poor match to the soft tissues and the curved, textured surfaces of the brain and the skin; they also often constrain and frustrate the dynamic, natural motions of these organs. Consequences include discomfort, irritation, and adverse immune responses at the critical interfaces (Grill et al., 2009; He and Bellamkonda, 2008; Polikov et al., 2005; Ward et al., 2009), thereby creating challenges in non-invasive initial integration and subsequent chronic operation. Furthermore, the basic architectures of the readout electronics do not scale effectively to the geometrical areas and the numbers of independent channels thought to be indispensable for recording neural data that span the dynamics of isolated neurons to individual neural circuits, to the entire brain. Such circumstances demand alternative materials, component devices, and functional systems for a next generation of neural interface technology.

This review summarizes recent progress in these directions, with an emphasis on approaches that embed soft materials and compliant mechanical structures in active electronic designs with potential to achieve spatiotemporal resolution across all relevant scales. The article begins with an overview of electrodes with unique capabilities in direct electrical interfaces to the surfaces or depths of the brain, and indirect ones through the skin. Subsequent sections illustrate means for combining such electrodes with electronic circuits capable of active, multiplexed readout, per-channel signal amplification, wireless transmission, and multimodal operation, in each case with representative neural data to illustrate the functional possibilities.

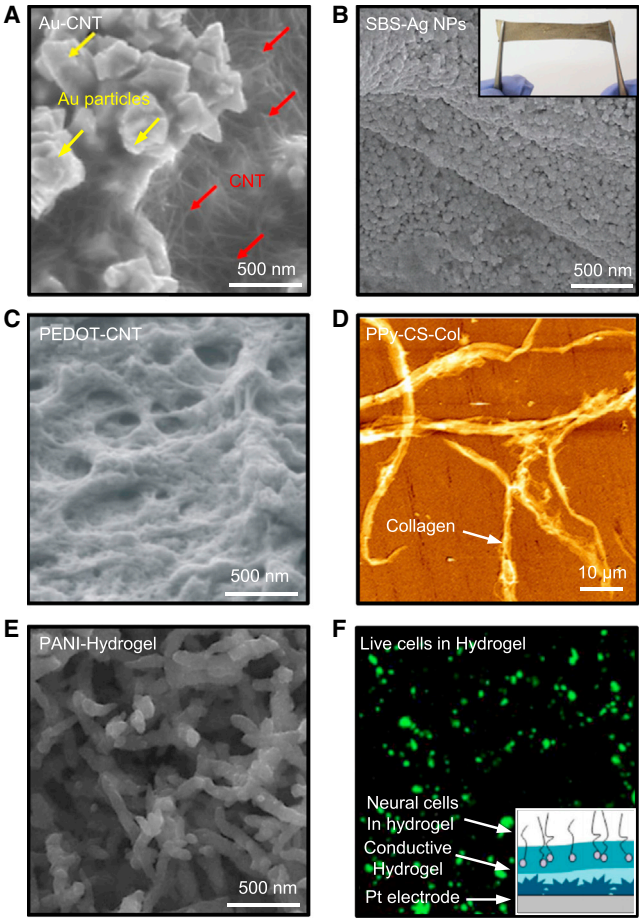

Figure 1. Soft Materials for Neural Interfaces

(A) Scanning electron micrograph of a percolating network of gold (Au) nanoparticles (yellow arrows) and carbon nanotubes (CNT, red arrows) in a polyimide matrix (Xiang et al., 2014).

(B) Scanning electron micrograph of a styrene-butadiene-styrene (SBS) triblock copolymer rubber with a percolating network of silver nanoparticles. The inset shows a picture of this material while stretched (Park et al., 2012).

(C) Scanning electron micrograph of a PEDOT/CNT composite. Electropolymerized PEDOT/CNT offers low impedance (15 kΩ with a diameter of 30 μm at 1kHz) compared to an Au electrode (330 kΩ with a diameter of 30 μm at 1kHz) (Gerwig et al., 2012).

(D) Atomic force micrograph of Polypyrrole (PPy)/chondroitin sulfate (CS)/collagen (Col) composite. Collagen fibrous matrix consists of small individual fibers of collagen with diameter of 150 to ~200 nm (Liu et al., 2011).

(E) Scanning electron micrograph of a polyaniline (PANI) / hydrogel composite. The dendritic nanofibers of PANI (~100 nm diameters) form a 3D interconnected network (Pan et al., 2012).

(F) Fluorescent optical micrograph of P12 neural cells in a sericin hydrogel (Green et al., 2013).

Soft, Compliant Neural Interfaces

Neural interfaces provide two-way communication between electronic devices and biological tissues for purposes of measurement and/or stimulation. The materials that serve as the electrodes play critically important roles, where interactions involve redistribution of charges (capacitive) and/or transfer of electrons and ions (Faradaic) at the double layer that forms between the electrode and electrolyte (i.e., surrounding biofluid) (Cogan, 2008; Merrill et al., 2005). The charge injection capacities and the impedances are generally thought to be most relevant to stimulation and sensing, respectively. Over the past 50 years, various metals, metal alloys, metal oxides, doped semiconductors, conductive polymers, and carbon nanomaterials have been explored. Platinum (Pt) and its alloys with iridium represent popular classes of metals, due to their chemical stability, bio-compatibility, and excellent electrical properties (Merrill et al., 2005; Petrossians et al., 2011). Here, Faradaic and capacitive mechanisms can be equally important, partly due to the modest injection capacity of Pt (0.05–0.15 mC/cm^2), as defined by the maximum amount of charge per unit surface area that can be delivered in the leading phase of a stimulation pulse, without causing irreversible electrochemical reactions. Another widely used material is iridium oxide, due to its capability for charge injection via fast, reversible Faradaic reactions (Mozota and Conway, 1983) associated with oxidation and reduction between multiple valence states of Ir in the oxide. Resulting capacities (1–5 mC/cm^2) can be greater than those of Pt (Merrill et al., 2005). Similar performance based on capacitive coupling within a regime of reversible electrochemical processes (Cogan, 2008) is possible with titanium nitride (TiN; ~1 mC/cm^2), also commonly used for neural electrodes. In all cases, texturing the electrode surfaces increases their areas, and therefore lowers the electrochemical impedance, with examples in porous TiN and sputtered iridium oxide (Cogan, 2008), and enhances the charge injection capacity (Petrossians et al., 2011).

Although these and other established materials are useful, they are mechanically hard (~50–500 GPa modulus, ~1%–5% elastic strain limit) and, in conventional forms, they offer shapes and structural properties that are highly dissimilar to those of targeted tissues. These and other drawbacks create interest in alternative, soft materials, such as conducting polymers and nanomaterial composites, which combine low modulus mechanics (1 MPa to 5 GPa modulus, 5%–500% elastic strain limit) and good biocompatibility (Asplund et al., 2009; George et al., 2005; Humpolicek et al., 2012) with an ability to be molded, printed or cast into complex, curvilinear shapes matched to tissues of interest, with or without additional nanotextures. These features facilitate integration on soft, moving biological surfaces with minimized inflammatory reactions and gliosis. Conducting polymers such as poly(3,4-ethylenedioxythiophene) (PEDOT) and polypyrrole (PPy), are attractive due to their low electrochemical impedances and high capacities (>15 mC/cm^2) (Cogan, 2008). Their modest conductivities can be addressed through the addition of nanomaterials to yield advanced composites that often also increase the active surface areas, without compromising the soft mechanics. Figure 1 shows some examples, including a dispersion of carbon nanotubes (CNTs) and gold nanoparticles in a polymer host (polyimide) (Figure 1A), silver nanoparticles in a soft elastomer (Figure 1B), and CNTs in a conductive polymer (Figure 1C) (Castagnola et al., 2014; Gerwig et al., 2012; Park et al., 2012; Xiang et al., 2014). In the first, electrodeposited nanoparticles decorate a 3D, percolating network of CNTs (Figure 1A) (Tsang et al., 2012; Zhang et al., 2014). The CNT/Au composite (< 100 kΩ for a 500 μm × 300 μm pad at 1 kHz) offers much lower impedances compared to those with Au (~1 MΩ for a 500 μm × 300 μm pad at 1 kHz) at all frequencies from 10 Hz to 100 kHz. The mechanics of this type of

composite can be further improved by replacing the polyimide with a low modulus elastomer, as shown in Figure 1B for the case of a poly(styrene-block-butadiene-block-sytrene) rubber (modulus 1 MPa, compared to ~kPa for biological tissue, 0.1–5 GPa for plastics) loaded with silver nanoparticles at a level that exceeds the percolation threshold. The resulting material offers high bulk conductivity even when stretched to strains of up to 100%. Replacing the nanoparticles with nanowires increases the conductivity, reduces the percolation threshold, and allows operation at strains of up to 450% and more (Lee et al., 2012), thereby far exceeding levels of deformation that occur naturally in neurological tissues. The electrical properties can be enhanced by use of matrix materials that are conducting (capacity of PEDOT/CNT >1 mC/cm^2). Electrodeposition, for example, provides a synthetic pathway to composites of PEDOT with CNTs or polymer nanotubes for brain machine interfaces (Abidian et al., 2010; Castagnola et al., 2014; Gerwig et al., 2012). Conducting polymers or CNTs can also be mixed with biological materials such as extracellular matrix (ECM) to form bioactive composites for increased cell adhesion, reduced inflammatory response, and accelerated growth rates as well as improved mechanical (low modulus) and electrical (low impedance) properties (Aregueta-Robles et al., 2014; Chan and Mooney, 2008; Chen and Allen, 2012). Chemically functionalized PPy with chondroitin sulfate (CS) provides functional groups for covalent attachment of biomolecules and can be formed into composites with collagen (Col) fibers to support cell adhesion and proliferation (340% higher cell numbers than PPy-CS at 168 hr) (Figure 1D) (Liu et al., 2011). Owing to their biocompatibility, ECM-based materials can reduce glial scarring and maintain low impedance.

Related composites can also be formed using hydrogels, of interest due to their ability to support stable ionic transfer for low electrical impedance and to present hydrophilic surfaces for minimized non-specific protein adsorption (Aregueta-Robles et al., 2014). Hydrogels can incorporate natural materials, such as collagen and alginate, or synthetic polymers, such as polyvinyl alcohol (PVA) and polyethylene glycol (PEG) (Lu et al., 2009; Rao et al., 2012). Copolymer hydrogels of PEDOT/PVA are notable due to their stable operation and high capacity (0.1 to ~2.5 mC/cm^2) (Aregueta-Robles et al., 2014). Figure 1E shows an example of a conductive polymer/hydrogel composite. Integrating living cells into hydrogels represents an interesting means to minimize foreign body response, where embedded neural cells survive as the hydrogel degrades to leave a natural matrix that blurs the boundary between the electronic and biological materials (Green et al., 2010; Green et al., 2013). Placing such a material on a Pt electrode coated with a conductive hydrogel (PEDOT/PVA/heparin) allows low resistance connection to external data acquisition systems. Figure 1F shows neural cells (PC12, Marinpharm) encapsulated in a PVA-sericin hydrogel on top of conductive hydrogel. The capacity (0.81 mC/cm^2) of this type of living cell electrode is similar to that of the PEDOT/PVA/heparin hydrogel (0.83 mC/cm^2); both are higher than that of Pt.

The match between the moduli of such hydrogels (0.1 to ~100 kPa) and those of the surrounding biomaterials represents an important feature, as also explored in stimuli-responsive softening polymer nanocomposites (Capadona et al., 2008; Ware et al., 2014). Ultimately, however, it is the mechanics at the level of the device structure that are paramount because they define the nature of interaction at the neural interface. For example, thick materials with low moduli can be less favorable than thin, appropriately designed structures of materials with high moduli. As a result, both the device architectures and the materials choices must be considered together in the engineering of a mechanically stable, minimally invasive technology. In particular, soft neural interfaces can be achieved using high modulus, inorganic active materials by forming them into optimized shapes and combining them with low modulus polymers. Here, thin, narrow structures offer effective moduli defined by bending motions, and by in- and out-of-plane rotations and translations that minimize the levels of strain in the constituent materials. The bending stiffnesses of micro/nanoscale wires, fibers, ribbons, and membranes can be exceptionally small, due to the cubic scaling of stiffness with characteristic dimension. Figure 2A shows the case of an electrode that consists of a carbon microfiber (~7 μm diameter) coated with an ultrathin (sub-micron thickness) layer of PEDOT. This structure can bend and flex easily, to accommodate natural pulsations and swelling/deswelling of the brain for accurate chronic recording of extracellular neural potentials from small groups of neurons (Kozai et al., 2012). Comprehensive mechanical and electrical studies indicate low impedance (~50 kΩ for a 38.5 μm^2 tip at 1 kHz), minimal damage to tissue associated with insertion, stable operation for more than 5 weeks, and much reduced formation of glial fibrillary acidic protein (GFAP), microglia or endothelial barrier antigen. Low stiffness (k, 4.5 × 10^3 N/m for a fiber with diameter of 8.5 μm and length of 2 mm c.f. 1.5 x 10^5 N/m for a standard silicon (Si) probe with thickness of 15 μm and length of 2 mm) and minimal insertion force are key characteristics.

The same principles apply to multifunctional classes of engineered fibers. The example in Figure 2B embeds a set of stimulating/recording electrodes with an optical waveguide for optical stimulation/interrogation and a microfluidic channel for drug delivery (Canales et al., 2015). Here, a thermal drawing process reduces the dimensions of a bulk, manufactured preform (cm's in diameter) by two orders of magnitude to produce long, thin multi-material fibers (85 μm diameter) that have bending stiffnesses (K, 4 to ~7 N/m for a fiber with length of 12 mm) that are ten times lower than those of steel wires (125 μm diameter) widely used in electrophysiology. The same principles apply to nanoscale materials such as Si nanowires (90 nm diameter) (Tian et al., 2010) and gold nanowires (~100 nm diameter) (Kang et al., 2014), which can form flexible interfaces with demonstrated use in recording of intracellular potentials from cardiac muscle cells and neural signals, respectively. Nanoribbons and nanomembranes of Si offer related mechanics, with the ability to serve not only as electrode interfaces, but also as active semiconductors in co-integrated electronics for signal multiplication and multiplexing, as described subsequently.

Although small dimensions lead naturally to bendability, effective integration with soft, deformable biological tissues demands stretchability, i.e., low modulus, elastic response to large strain deformations. Achieving this outcome with hard, high performance electronic materials requires concepts beyond

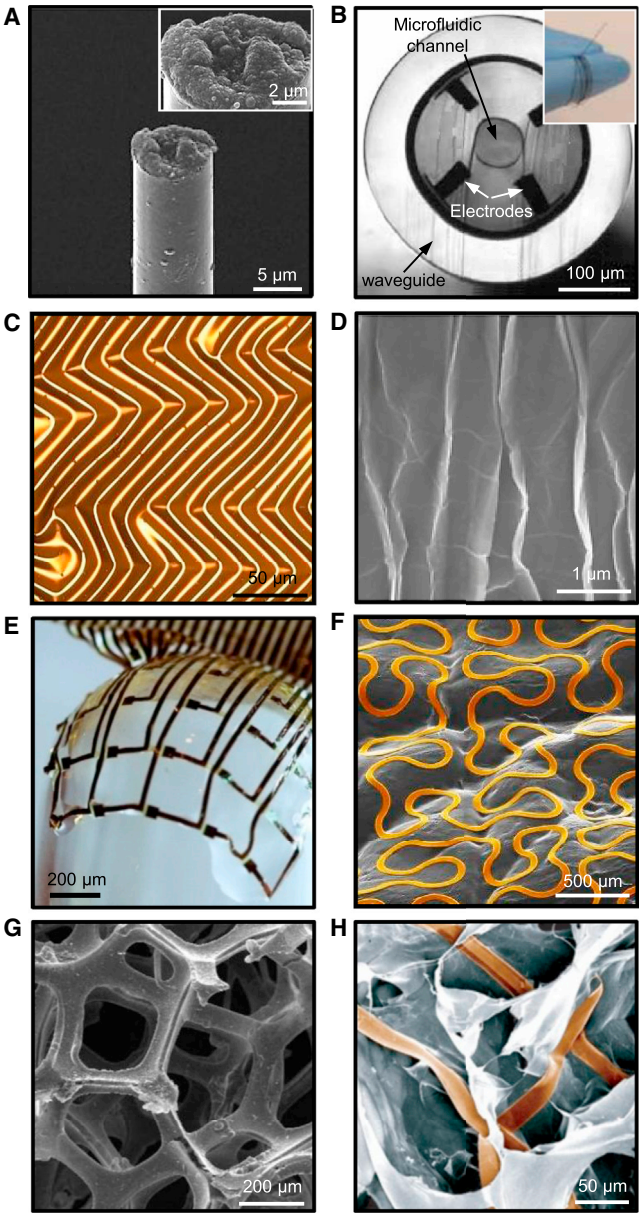

Figure 2. Soft Structures for Neural Interfaces

(A) Scanning electron micrograph of the tip of an electrode that consists of a carbon fiber (8.5 μm diameter) coated with PEDOT. The materials, geometry, and mechanics minimize damage associated with insertion, yield low interface impedance, and enable chronic recordings (Kozai et al., 2012).

(B) Scanning electron micrograph of a multi-material functional fiber device that embeds recording electrodes, microfluidic channels, and optical waveguides. The inset shows a photograph of the fiber wrapped around the index finger to illustrate its mechanical flexibility (Canales et al., 2015).

(C) Optical image of a two-dimensional wavy silicon nanomembrane on a soft silicone substrate. This geometry imparts an effective stretchability and low modulus mechanics to the silicon, which is a brittle, hard material (Choi et al., 2007).

(D) Scanning electron micrograph of a wavy structure of graphene on a rubber substrate. This system can be stretched to strains of up to 450% without noticeable change in the electrical conductivity (Zang et al., 2013).

(E) Photograph of an electrode array in an open mesh geometry wrapped onto the hemispherical tip of a glass rod. This ability to conform to curvilinear surfaces enables accurate neural recordings from the surface of the brain (Kim et al., 2010).

(F) Scanning electron micrograph of a conducting, open mesh with a fractal-inspired geometry constructed using Peano curves, resting on a substrate with the surface texture of skin. Such constructs enhance contact between electrodes and the surfaces of biological tissues (Fan et al., 2014).

(G) Scanning electron micrograph of a 3D scaffold of graphene. These platforms can serve as active, 3D scaffolds for neural stem cells (Li et al., 2013).

(H) Scanning electron micrograph of a 3D silicon nanowire mesh in a matrix of alginate. This construct provides a route for integrating hard electronic materials with soft, 3D biological systems (Tian et al., 2012).

reductions in key dimensions. One widely explored route exploits controlled buckling processes to form "wavy" shapes in hard micro/nanomaterials bonded to the surfaces of soft elastomeric substrates (Kim et al., 2012; Rogers et al., 2010). The response of this type of structure, which can be considered as an engineered, or deterministic, composite material, to applied strain involves a physics that is related to that of an accordion bellows, in which the elastomer provides the restoring force and defines the effective modulus. Figure 2C shows this idea embodied in a wavy silicon nanomembrane (100 nm thickness) on a silicone substrate (Choi et al., 2007). Similar strategies apply equally well to many other materials, including graphene, as illustrated in Figure 2D (Zang et al., 2013). This example exhibits excellent electrical conductivity even under tensile strains of up to several hundred percent. Structuring the materials into open mesh layouts further enhances the mechanics, as shown in Figure 2E with an image of an ultrathin neural electrode array wrapped onto the hemispherical end of a glass rod (Kim et al., 2010). Complete, conformal integration onto this type of non-developable shape, as for nearly any surface found in biology, requires stretchability and cannot be accomplished with bending alone. In vivo studies of the visual cortex of a feline animal model demonstrate that the accuracy and reliability of recordings performed with electrode arrays in thin mesh architectures greatly exceed those possible with otherwise identical arrays in uniform, thin film formats (Kim et al., 2010). Advanced mesh designs involve ideas in fractal geometry (Fan et al., 2014) as shown in Figure 2F, and described subsequently. Extension to full, 3D layouts presents challenges in fabrication but offers wide ranging modes of deformation and volumetric integration with cells. 3D open architectures of graphene synthesized on the surface of a porous nickel (Ni) foam, followed by removal of the Ni by selective etching, (Chen et al., 2011) provide compliant structures that can support neural stem cell growth (Figure 2G). Related types of 3D materials include silicon nanowire scaffolds with macroporous layouts (Tian et al., 2012) that offer integrated sensory capabilities for recording both extracellular and intracellular signals in 3D cultures of neurons (Figure 2H). Such biocompatible hybrid structures can mimic certain properties of natural tissue scaffolds.

Surface Conformal Neural Interface Systems

Electrocorticography (ECoG) and electroencephalography (EEG) represent two modes in which the materials described in the previous sections can be used to monitor and stimulate electrical activity in the brain. The capacity for conformal contact over large, curvilinear surfaces that are time varying in their shapes, potentially extending to the entire scalp (EEG) or cortical surface (ECoG), and integrated electronics for amplified, multiplexed

readout represent emerging capabilities of direct relevance to the long-term goals of the Brain Activity Map project (Alivisatos et al., 2013), as described in the following.

EEG involves measurements using arrays of electrodes applied to the scalp, as first explored 90 years ago (Adrian and Matthews, 1939; Collura, 1993). Despite some notable technical improvements (Debener et al., 2012; Wolpaw and McFarland, 2004), modern systems for EEG still require separately wired bulk electrodes made of conventional metals, interfaced to the scalp using conducting pastes or gels. Disadvantages include (1) inability to perform chronic recordings (more than a few hours) due to drying and/or other forms of degradation of the pastes/gels; (2) lack of a comfortable, mechanically stable interface to the skin; and (3) time-consuming, cumbersome manual procedures for mounting the electrodes. Recent advances in materials, structural interfaces, integration schemes, and data acquisition systems create opportunities to overcome these limitations. For example, cross-linked sodium polyacrylate hydrogels swelled with electrolyte can serve as soft electrodes for low impedance (compared to commercial electrodes) conformal interfaces to the skin, including hair bearing regions (Alba et al., 2010). A high solution content (>90% by weight) allows these materials to be used for more than 24 hr under normal laboratory conditions. Dry polymer-based electrodes, such as those constructed with thin layers of PEDOT:PSS on films of polyimide, avoid evaporative degradation entirely, to yield stable interfaces that can also mechanically flex to follow the curved surfaces of the head (Leleux et al., 2014). Recent reports suggest an ability of such electrodes to capture EEG waveforms that are not easily resolved using conventional materials (Chen et al., 2013; Fiedler et al., 2011). Other emerging classes of dry electrodes exploit conductive elastomeric composites like those described previously to provide further enhanced conformality and adhesion to the skin (Jung et al., 2012). Their permeability to gas/moisture allows for natural processes of transepidermal water loss to facilitate long-term measurements, as recently demonstrated in studies of ECG (electrocardiography).

An alternative composite strategy combines inorganic electronic materials deterministically shaped into micro/nanostructures and embedded in soft elastomeric matrices to yield integrated collections of devices that include not only EEG electrodes but also multifunctional sensors (such as temperature, strain, and electrophysiological), active/passive circuit elements (such as transistors, diodes, and resistors), wireless power coils, and components for radiofrequency communications (such as high-frequency inductors, capacitors, oscillators, and antennas) (Kim et al., 2011). Fabrication approaches that exploit methods used in the semiconductor industry afford a precision in design that allows such systems to be engineered with effective physical characteristics (thickness, area mass density, elastic modulus, thermal properties, stretchability) that match those of the epidermis itself. The result is a technology, sometimes referred to as epidermal electronics, that can softly laminate onto the surface of the skin, to allow non-irritating, low impedance, stable electrophysiological measurements for up to 2 weeks (Yeo et al., 2013), without any significant mechanical constrain on natural motions or processes (e.g., transepidermal water loss). Figure 3A, left and center, shows systems of this type. The layouts involve open, serpentine filamentary mesh structures of active electronic materials (i.e., Si, GaAs, or metals) encapsulated by thin layers of polyimide (1.2 μm thick) and embedded in a low modulus, gas/moisture permeable silicone elastomer. Concepts in fractal-inspired geometry (Peano as in Figure 2F, Koch, Hilbert, Moore, Vicsek and others) yield arrays that can cover areas at scales comparable to those of the entire skull (Figure 3A, left), with individual electrode sizes at sub-millimeter dimensions, in interconnected networks with nearly any geometry (Fan et al., 2014). The absence of closed loop current pathways in appropriately selected fractal curves affords invisibility under magnetic resonance imaging (Fan et al., 2014). Figure 3A (center) shows the process of gently peeling an epidermal electronic system from the forehead after use. High-quality EEG data can be acquired over many days, continuously, without removing or re-mounting the devices. Thin fabrics can be included as backing layers to improve the mechanical robustness, thereby allowing multiple cycles of use, cleaning, and sterilization (Jang et al., 2014). The data in Figure 3A (right) illustrate alpha rhythms that appear in an awake subject when the eyes are closed (Kim et al., 2011). The signal-to-noise ratios are comparable to those possible using conventional, rigid bulk electrodes with conductive coupling gels.

These concepts in open mesh structures and fractal geometries allow integration of customized, ultrathin semiconductor devices for local signal amplification, multiplexed readout, and wireless communications. Alternative designs use sealed microfluidic chambers and "origami-like," deformable electrical interconnects to enable use of state-of-the-art, chip-scale components in a manner that does not compromise the soft, low modulus mechanics of the overall system (Xu et al., 2014). Figure 3B (left) shows a wirelessly powered device with radio frequency communication capabilities in a twisted shape. Using this technology with the types of soft, mesh electrodes shown in Figure 3A allows tether-free operation in EEG. The results (Figure 3B, center and right) demonstrate signals that are quantitatively consistent with those collected using wired acquisition systems and hard electrodes.

The technologies of Figure 4 incorporate classes of active electronics needed for local amplification and multiplexed readout of measured signals. These features, taken together with the scalability of the fabrication schemes, allow measurement at hundreds, with the potential of millions, of electrode sites with a single conformal system. Such capabilities are of particular importance in the context of ECoG, and advanced forms sometimes referred to as microscale ECoG (μECoG), where an ambitious goal is to measure potentials across the entire cortical surface at an oversampled spatial resolution of a few tens of microns. This mode of operation demands hundreds of millions of actively addressed electrodes, each with local, per-channel signal amplification. Figure 4A shows a system that represents progress in this direction, where silicon nanomembranes (260 nm thick) support semiconductor device functionality (720 transistors) with performance characteristics similar to those found in conventional, wafer-based electronics, for readout across an array of nearly four hundred electrodes (300 × 300 μm^2 with 500 μm spacing) (Viventi et al., 2011). The spatial resolution of the most advanced μECoG systems of this type

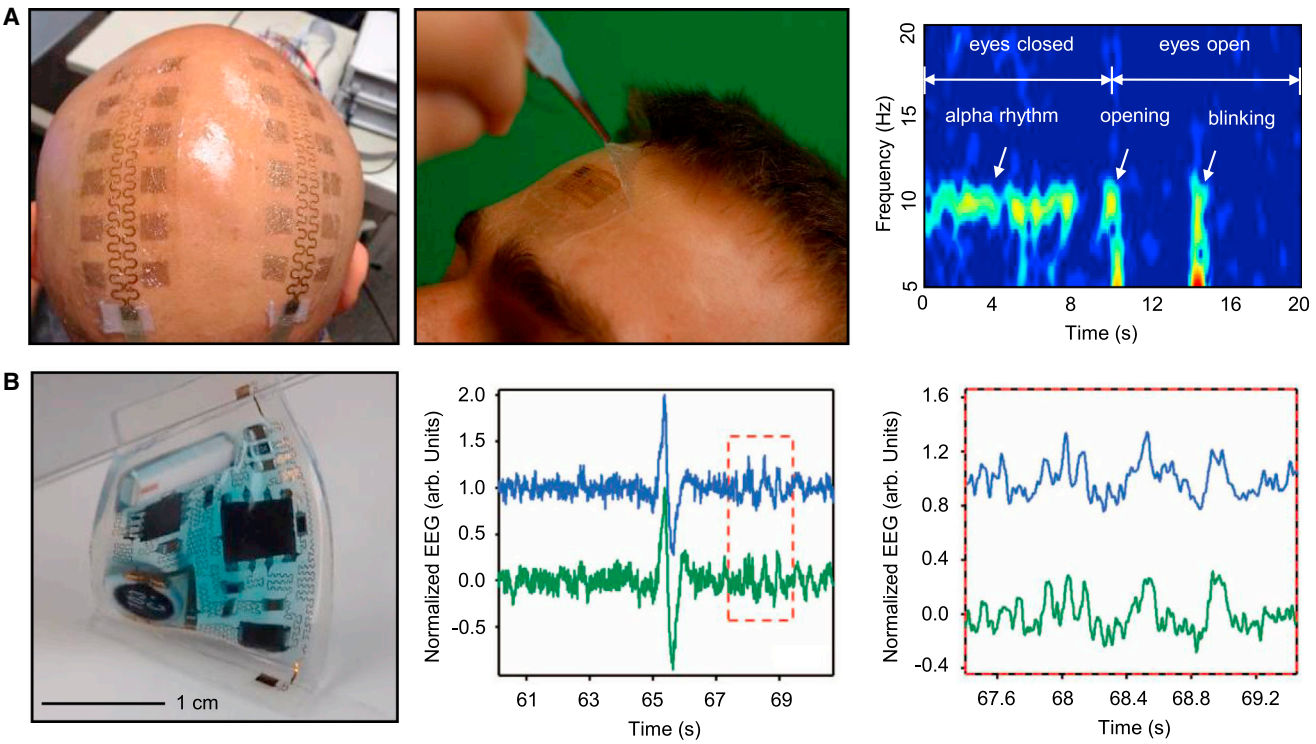

Figure 3. Soft, Conformal Electronics for EEG

(A) Images of skin-like, or epidermal, electronics that exploit electrodes and semiconductor components in open, filamentary mesh architectures with fractal inspired geometries (left). These devices can softly laminate onto and peel away from (middle) the surface of the skin for stable, non-irritating, long-lived measurement interfaces. Spectrograms of representative EEG data (right) show characteristic alpha rhythm behavior when the eyes are closed (Kim et al., 2011). (B) Image of a stretchable electronic system that integrates chip-scale components and a free-floating interconnect network for wireless EEG. Data acquired from the forehead (green; middle and right) are quantitatively similar to those simultaneously acquired using a wired commercial device (blue). The large deflections correspond to blinking of the eyes as the subject shifts from performing mental math to resting (Xu et al., 2014).

(Escabí et al., 2014) is nearly sixteen hundred times finer in terms of electrodes per unit area than that of passive, clinical ECoG devices, thereby reaching levels that even exceed those associated with much smaller, rigid penetrating Si microneedle systems. Mechanical flexibility follows from the thin geometries of the functional materials, to allow not only mounting on the gyral surfaces but also, through sharp bending, insertion into the sulci and the interhemispherical spaces (Figure 4B) (Viventi et al., 2011). The electrical design incorporates buffering and multiplexing transistors at each unit cell, for per-channel sampling rates of >10 kS/s with low cross-talk (<−65 dB) and only 39 wires for data acquisition. This architecture offers nine times fewer wires than that required for a passive system with equivalent layout; for a device with one million measurement sites, this advantage grows to a factor of 500. The electrodes themselves consist of thin films of platinum on the top, outer surface of a multilayer assembly of conductors, insulators, and semiconductors that forms the electronics, supported by a flexible sheet of polyimide. Amplifying capabilities can be easily included at each channel, to improve further the levels of performance, as recently demonstrated in epicardial mapping systems (Viventi et al., 2010).

Figure 4C shows an example of the use of this active μECoG technology to reveal the electrical dynamics associated with a seizure induced in a feline model, at high spatial and temporal resolution. The signal from each channel in the array exhibits large amplitude (>6 mV), low noise (<45 μV root-mean-square deviation), and high signal-to-noise ratio (34 dB). The spatio-temporal patterns of activity shown in Figure 4C begin with an ictal onset that corresponds to a plane wave originating from the upper left. An anisotropy bends the wave to the right, thereby launching a clockwise spiral pattern that persist for three rotations. A second plane wave then emerges to change rotation direction to counterclockwise. This behavior continues for 19 cycles and ends with termination by a plane wave that comes from the right. Such spatio-temporal responses, uniquely observable with the systems described here, have qualitative features that are reminiscent of those associated with cardiac arrhythmias. This information provides important insights into the nature of neocortical seizures, with potential relevance to understanding and treatment of brain disorders such as epilepsy. Additional studies using such μECoG devices, but with further improved spatial resolution, on the auditory cortex exhibit quantitative agreement with much slower measurements performed using intrinsic optical imaging (Escabí et al., 2014).

The requirements in active multiplexing and amplification impose performance demands in flexible electronics that can only be satisfied with nanostructured inorganic semiconductors such as the Si nanomembranes used in the previously described systems. Organic and composite electronic materials do,

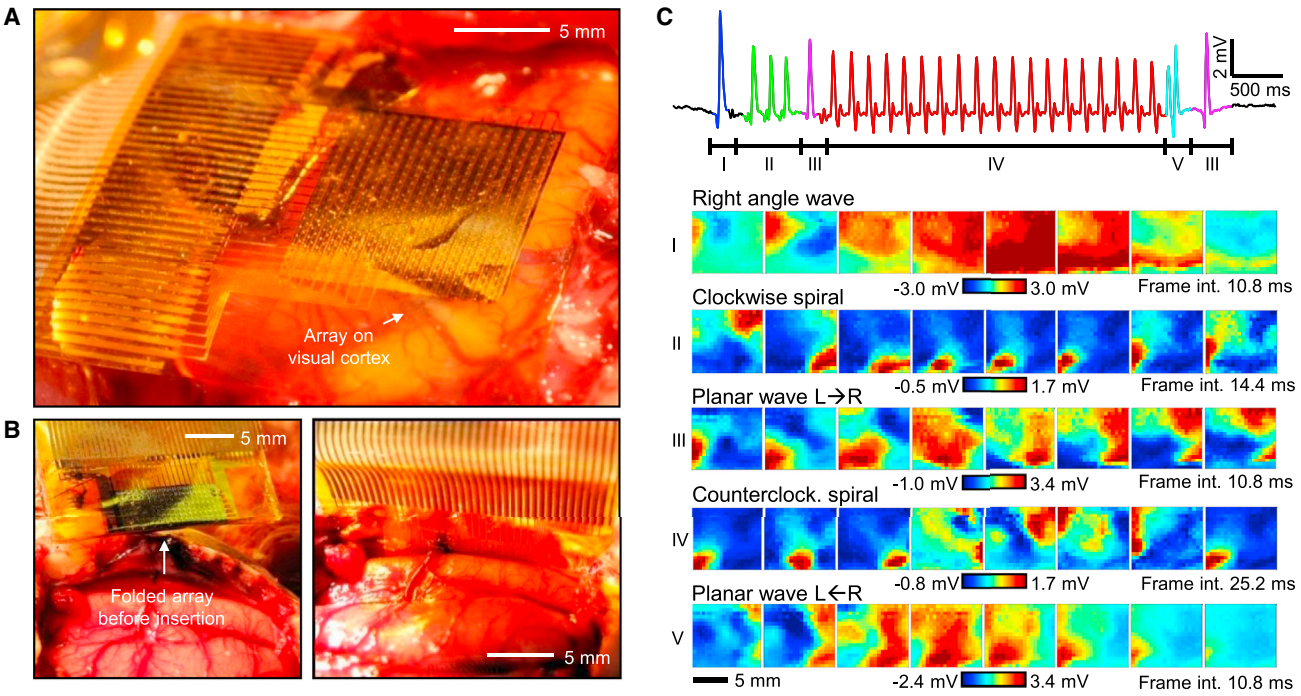

Figure 4. Actively Multiplexed Flexible Electronics for μECoG
(A) Image of a device placed on the cortical surface of a feline model.
(B) Image of a similar device folded to allow insertion into the interhemispheric fissure (left) and after insertion (right).
(C) Measured μECoG signal from a representative channel of a device during an electrographic seizure. The labeled segments correspond to maps of electrical potential that illustrate the spatio-temporal dynamics, as shown in the frames below (Viventi et al., 2011).

however, have potential utility as electrode interfaces to the brain in systems that use this type of electronics. PEDOT represents an example that shows promise in ECoG measurements (Khodagholy et al., 2011). As incorporated into electrochemical transistors, PEDOT offers enhanced signal levels due to local amplification, with information content similar to that obtained using penetrating electrodes. Other recent work suggests that transparent flexible electrodes based on graphene (Kuzum et al., 2014) and inorganic alternatives such as indium tin oxide (Ledochowitsch et al., 2011), can offer excellent measurement capabilities with options in simultaneous optical imaging or stimulation. Future directions include efforts to render ECoG measurement capabilities in systems that are not only flexible, but also stretchable, as demonstrated recently in passive electrode arrays based on polypyrrole/polyol-borate composites (Guo et al., 2014).

Soft Penetrating Neural Interface Systems

Neural interfaces based on compliant, thin sheets of electrodes can minimize physiological reactions such as local inflammation and scar formation by conforming to biological surfaces and minimizing mechanical loads on them. Direct measurements into the depths demand other approaches, such as neural probes that penetrate targeted tissues. Traditional systems incorporate micromachined arrays of Si needles (typically 100, each with 10–30 μm diameters on a 400 μm pitch) on planar silicon platforms (500 μm thick), or grid patterns of electrodes (as many as 256, each with an area of 400 μm^2 on a 50 μm pitch) on polyimide sheets (5 μm thick) (Wise et al., 2008). Progress outlined here allows active, multifunctional device functionality in ultraminiaturized form factors that can, through their mechanical compliance, reduce tissue damage upon insertion and chronic use, the latter partly due to an ability to move with natural pulsations, patterns of swelling/deswelling, and motion of the brain within the intracranial space. One simple example exploits the carbon fiber platform of Figure 2A in which a thin poly(p-xylylene) layer serves as a dielectric for a PEDOT coated electrode of poly(thiophene) (Kozai et al., 2012). The result is an electrode that is one order of magnitude smaller in diameter (~7 μm) than conventional devices, with a bending stiffness reduced by a corresponding amount. Adequate signal levels are possible even with small cross-sectional areas (~60 μm^2 compared to ~300–3000 μm^2 for standard Si probes) due to the low interface impedances enabled by the polymeric conductors. Such an interface is suitable for chronic recordings of single-neuron activity, with sufficient signal to noise (~5–10) for measurement of potentials as small as a few tens of microvolts, as demonstrated in the motor cortex of rat in Figure 5A. In addition, separate manipulation of each probe provides some flexibility in location, although with a loss in parallelism of the mounting process, compared to standard probe arrays.

Further reductions in the dimensions of probes such as these lead to bending stiffnesses that are insufficient for insertion into the brain tissue. This limitation can be avoided with materials that temporarily provide mechanical strength for insertion, but then disappear by processes of bioresorption (Wu et al., 2011,

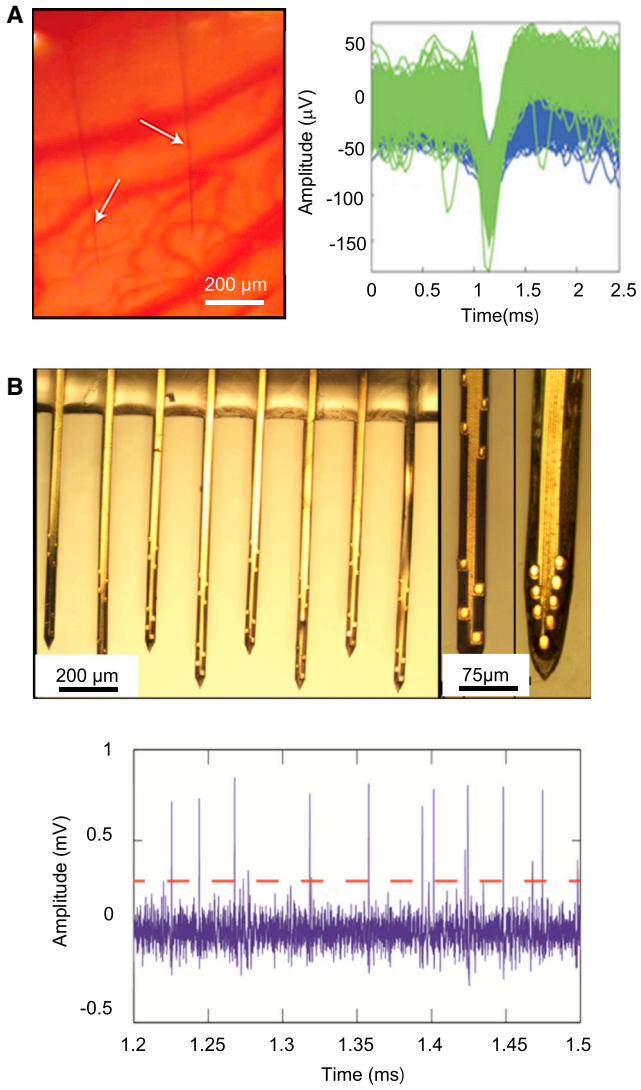

Figure 5. Flexible, Minimally Invasive Penetrating Neural Probes

(A) Image of a pair of carbon fiber based microprobes inserted into the cortex of rat (left) and representative recording results (right) of single neural activity over 2.5 min (Kozai et al., 2012).

(B) Image of a flexible neural probe coated with a film of silk fibroin (left), with a magnified view of two of the probes (right) and a representative recording result from the layer five of rat motor cortex (bottom). The red dotted line represents the threshold for spike detection (Wu et al., 2013a).

2013a). The physical properties (Young's modulus of 4–6 GPa, >80% elongation at break), easy processability (casting, molding), and established bioresorption characteristics of silk fibroin make it an attractive choice for this purpose (Tien et al., 2014). In one case, a coating (65 μm thickness) of silk encapsulates a small array of eight penetrating needles, each of which has eight planar electrodes built on a thin, flexible film of polyimide (5 μm thickness). Figure 5B shows such a device, and some representative data. These spike waveforms correspond to activity at layer five of the rat motor cortex, and the red dotted line represents the threshold for spike detection in 20 min recording sessions for 5 weeks. Aside from biodegradable or injectable substrates, these soft penetrating neural interface systems benefit from fabrication methods adopted from the microelectromechanical systems community (Rubehn et al., 2013). We expect continued progress in the development of new materials for these neural interface systems and the translation of these technologies toward clinical implementation.

Recent advances in materials and fabrication techniques afford the ability to incorporate multifunctional, active operation into compliant, neural probes. The resulting set of capabilities extends well beyond simple electrical functionality to include fluid delivery/extraction, optical stimulation/inhibition, simple spectroscopic characterization, thermal sensing, and many others. Such modes of interaction can help to reveal the simultaneous chemical, electrical, and mechanical signaling associated with the complex nature of neural circuit dynamics. Figure 6A provides an example that builds on the multimaterial fiber structures introduced in Figure 2B (Canales et al., 2015). Here, the fiber consists of a hollow channel responsible for drug delivery, an optical cladding layer of poly(etherimide) (PEI) layer, a sacrificial layer of poly(phenylsulfone) (PPSU), and a collection of Sn microelectrodes. The electrodes allow for neural recordings; the hollow channel enables delivery of neuromodulatory compounds; and the PEI and PPSU bi-layer forms an optical waveguide for light delivery and optogenetic stimulation. The resulting multimaterial structure provides a highly flexible (Figure 6A, middle) multifunctional neural interface with sub-micron feature sizes. An essential feature of this device is its ability to introduce light for optogenetic control over activities of individual neurons within neuronal populations of living tissues (Boyden et al., 2005), while retaining essential capabilities in electrical measurement. Figure 6A, right, shows evoked neural activity correlated with optical stimulation (5 ms pulse width at 20 Hz, for 1 s) in the prefrontal cortex in a Thy1-ChR2-YFP mouse. These hybrid probes, sometimes known as optrodes, represent powerful platforms for experimental neuroscience (Anikeeva et al., 2012; Wu et al., 2013b; Ozden et al., 2013).

Fully integrated, 'cellular-scale' injectable optoelectronic systems might represent an ideal class of technology for penetrating neural probes. Recent developments in materials science, mechanical engineering, and manufacturing methods allow construction of wide ranging classes of semiconductor devices and sensors in this format, along with their integration onto ultrathin, filamentary polymer supports. Figure 6B presents images that illustrate the multilayer layout of a representative system that combines arrays of light emitting diodes (microscale inorganic light emitting diodes, μ-ILEDs; InGaN, 6.4 μm thick, 50 × 50 μm^2) co-located with optical detectors (microscale inorganic photodiodes, μ-IPDs; silicon, 1.25 μm thick, 200 × 200 μm^2), and thermal and electrophysiological sensors and actuators (Kim et al., 2013). Bonding to a releasable injection microneedle using silk fibroin provides the necessary rigidity and physical toughness for penetration into the brain. Miniaturized wireless powering modules and control schemes enable remote, untethered operation. Such systems deliver electrophysiological and optoelectronic function directly to controlled locations in the depth of the brain without lasers, optics, fiber coupling systems, or optomechanical fixturing hardware used in traditional optogenetics approaches. The cellular-scale dimensions of the components,

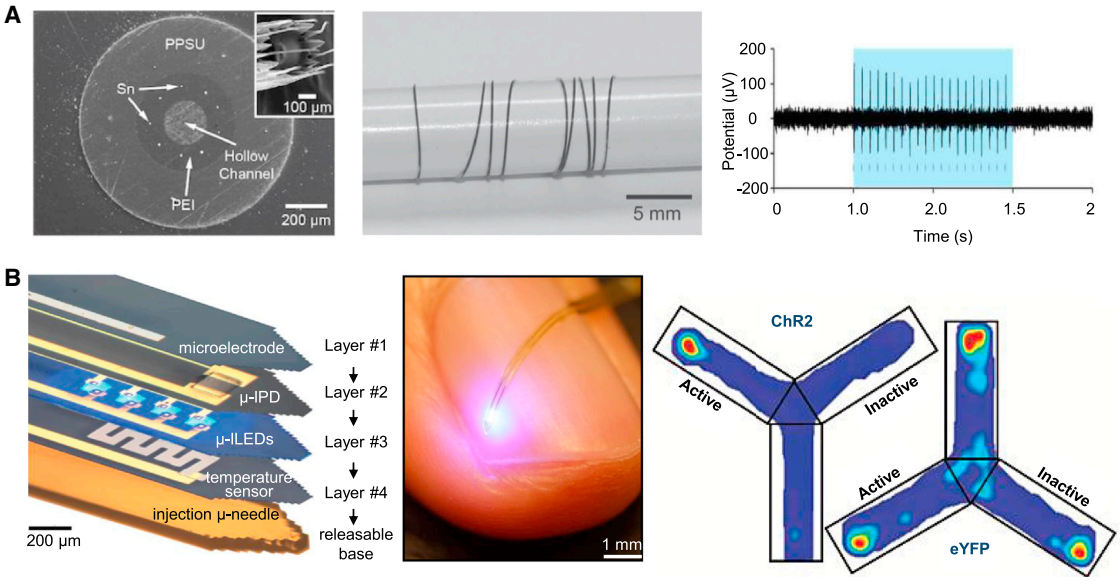

Figure 6. Flexible, Multifunctional Systems for Electrical, Optical, and Thermal Stimulation and Recording

(A) Scanning electron micrograph of a multifunctional fiber probe. A cladding layer of poly(etherimide) (PEI) surrounds a hollow channel that allows for drug delivery, nine electrodes of Sn incorporated into the PEI layer enable neural recordings, and the PEI and a sacrificial poly(phenylsulfone) (PPSU) layer permit optogenetic stimulation (left). The inset shows exposed Sn electrodes after etching of the cladding. Photograph of the fiber wrapped around the shaft of a pencil to illustrate its mechanical flexibility (middle), and representative electrical recordings during optogenetic stimulation of neuronal populations in the prefrontal cortex (right). The region highlighted in blue represents the time during optogenetic stimulation (5 ms pulse width, at 20 Hz for 1 s) (Canales et al., 2015).

(B) Optical micrograph that illustrates the multilayered construction of an injectable, cellular-scale optoelectronic device that includes microelectrodes, microscale inorganic photodetectors (μ-IPDs), microscale inorganic light emitting diodes (μ-ILEDs), and temperature sensors, bound to a releaseable injection microneedle (μ-needle) with a thin, bioresorbable film of silk fibroin (left), an image of such a device draped across the a fingernail (middle), and heat maps of activity of a mouse model in the Y-maze with conditioned place preference; hotter colors represent longer duration in the same position (right) (Kim et al., 2013).

the compliant mechanics, and the favorable thermal characteristics are all critically important for minimizing adverse biological responses in long-term use. Quantitative experimental study reveals substantially less glial activation and smaller lesion sites as compared to both metal cannulae and fiber optics, at both early (2 weeks) and late (4 weeks) phases. Low temperature operation follows from (1) highly efficient thermal spreading that results from the large surface area to volume ratios associated with the μ-ILEDs, (2) thermal sinking provided by natural blood flow in the vasculature of the surrounding tissue, and (3) minimized thermal generation due to efficient, low duty cycle, pulsed mode operation of the μ-ILEDs. The peak operating temperatures are in the range of 0.1°C, significantly below values that are known to cause unwanted effects in brain tissue.

These devices enable traditional optogenetics experiments as well as those that involve social interactions, complex 3D environments and other conditions that are incompatible with tethered operation and fiber optic delivery. In one feasibility demonstration, wireless control of μ-ILEDs injected into animals that express a channel rhodopsin in the locus coeruleus, a brain region with known longitudinal noradrenergic cell bodies, leads to activation of dopaminergic neurons. The optogenetic stimulus is sufficient to train complex behaviors using only wirelessly triggered illumination from the μ-ILEDs, without any physical reward. The activity maps in Figure 6B (right) show that such optogenetic conditioning can lead to a place-preference in a simple Y-maze. Such technologies offer strong potential not only for future optogenetics experiments, but also, through deep tissue injection of heterogeneously integrated optoelectronic systems, for accelerated progress in many areas of basic neuroscience and clinical treatment methods.

Concluding Thoughts

Scientific and engineering advances are rapidly adding to the toolbox of available hardware and measurement approaches for research in neuroscience. Soft interface technologies create new opportunities in measurement/stimulation that derive from unique options in noninvasive, conformal integration with the soft, curved surfaces and the compliant, heterogeneous depths of biological tissues. An important perspective is that, in many cases, such electrical systems can be converted into sophisticated biomolecular sensors by chemically functionalizing the electrode surfaces. Examples include electrodes formed from conducting polymers (Gerard et al., 2002; Guimarda et al., 2007), organic/inorganic nanomaterials including silicon nanowires (Cui et al., 2001; Patolsky and Lieber, 2005; Zheng et al., 2005), carbon nanotubes (Chen et al., 2003; Jacobs et al., 2010; Wang, 2005), and graphene (Wang et al., 2011). The scalability of the embedded electronics and diverse options in multifunctional operation create a rich range of promising directions for further development. The fabrication procedures and materials associated with several of the devices described here align well with those of the consumer electronics industry, thereby offering leverage for further accelerated rates of improvement in

performance and scale. Here, transistors, light-emitting diodes, photodetectors, electrodes, and interconnects can be formed at sub-micron dimensions, in multilayered formats, with levels of integration that approach billions of devices, over areas of hundreds of square centimeters. Adapting and repurposing this set of manufacturing capabilities for use in neural interfaces will be essential to their widespread use in the neuroscience community. A key challenge for chronic applications is that unlike conventional systems of implantable electronics where titanium casings can serve as hermetic enclosures, soft and flexible devices demand similar levels of hermeticity from thin, flexible layers of materials.

These technologies offer powerful modes of operation not only in the context of the brain, but also in other parts of the central nervous system and in the peripheral nervous system as well. A recent example is in the demonstration of soft neural interface devices, including ultra-compliant microelectrode arrays that insert into the epidural space and accommodate movement of the spinal cord (Minev et al., 2012; Minev et al., 2015), while providing essential recording and stimulating function in the context of regenerative medicine. Co-integration of fluidic and optical components in these systems, and scaling of their area coverage and resolution via multiplexed electronics will offer the same sorts of expanded capabilities as those for brain interfaces described here. In all cases, an exciting and ambitious future goal is to develop strategies that allow intimate, distributed 3D integration of these sorts of neural interface devices with tissues of interest. Combining the capabilities of such new approaches with other emerging methods in nanotechnology, fMRI, molecular/cellular optical imaging techniques, and chemical sensors will be essential to the pursuit of a full understanding of brain function.

Finally, we note that, beyond their use for research, the types of technologies described here have significant potential utility in clinical medicine, ranging from diagnostic systems for the surgical treatment of epilepsy to modulatory devices for the mitigation of symptoms of Parkinson's disease. Continued development of unusual materials, such as modulus-changing polymers (Ware et al., 2014) and shape and/or compositionally engineered diamond (Edgington et al., 2013; Hopper et al., 2014), and device concepts, such as wirelessly communicating neural micro-sensor "dust" (Seo et al., 2014), may yield further advances. Accelerated commercial translation will be essential to adoption of any emerging technology in clinical contexts. Challenges, even for systems with demonstrated utility, range from the formulation of thin, compliant materials that can serve as long-lived barriers to biofluids to the establishment of advanced manufacturing techniques for reliable, large-area production of systems that combine dissimilar classes of hard and soft materials in micro and nanostructured forms. To facilitate solutions, additional work is needed to establish a basic understanding of the long-term performance and biocompatibility of neural interfaces based on soft materials and structures. Compelling broader prospects in science and technology, together with the specific, immediate opportunities to expand our knowledge of the brain and our range of clinical treatment procedures conspire to create many promising, multidisciplinary directions for future work.

REFERENCES

Abidian, M.R., Corey, J.M., Kipke, D.R., and Martin, D.C. (2010). Conducting-polymer nanotubes improve electrical properties, mechanical adhesion, neural attachment, and neurite outgrowth of neural electrodes. Small *6*, 421–429.

Adrian, E.D., and Matthews, B.H.C. (1939). The Berger rhythm: potential changes from the occipital lobes in man. Brain. J. Neurol. *57*, 355–385.

Alba, N.A., Sclabassi, R.J., Sun, M., and Cui, X.T. (2010). Novel hydrogel-based preparation-free EEG electrode. IEEE Trans. Neural Syst. Rehabil. Eng. *18*, 415–423.

Alivisatos, A.P., Chun, M., Church, G.M., Deisseroth, K., Donoghue, J.P., Greenspan, R.J., McEuen, P.L., Roukes, M.L., Sejnowski, T.J., Weiss, P.S., and Yuste, R. (2013). Neuroscience. The brain activity map. Science *339*, 1284–1285.

Anikeeva, P., Andalman, A.S., Witten, I., Warden, M., Goshen, I., Grosenick, L., Gunaydin, L.A., Frank, L.M., and Deisseroth, K. (2012). Optetrode: a multichannel readout for optogenetic control in freely moving mice. Nat. Neurosci. *15*, 163–170.

Aregueta-Robles, U.A., Woolley, A.J., Poole-Warren, L.A., Lovell, N.H., and Green, R.A. (2014). Organic electrode coatings for next-generation neural interfaces. Front Neuroeng *7*, 15.

Asplund, M., Thaning, E., Lundberg, J., Sandberg-Nordqvist, A.C., Kostyszyn, B., Inganäs, O., and von Holst, H. (2009). Toxicity evaluation of PEDOT/biomolecular composites intended for neural communication electrodes. Biomed. Mater. *4*, 045009.

Boyden, E.S., Zhang, F., Bamberg, E., Nagel, G., and Deisseroth, K. (2005). Millisecond-timescale, genetically targeted optical control of neural activity. Nat. Neurosci. *8*, 1263–1268.

Campbell, P.K., Jones, K.E., Huber, R.J., Horch, K.W., and Normann, R.A. (1991). A silicon-based, three-dimensional neural interface: manufacturing processes for an intracortical electrode array. IEEE Trans. Biomed. Eng. *38*, 758–768.

Canales, A., Jia, X., Froriep, U.P., Koppes, R.A., Tringides, C., Selvidge, J., Lu, C., Hou, C., Wei, L., Fink, Y., and Anikeeva, P. (2015). Multimodality fibers for simultaneous optical, electrical and chemical communication with neural circuits In vivo. Nat. Biotechnol. http://dx.doi.org/10.1038/nbt.3093.

Capadona, J.R., Shanmuganathan, K., Tyler, D.J., Rowan, S.J., and Weder, C. (2008). Stimuli-responsive polymer nanocomposites inspired by the sea cucumber dermis. Science *319*, 1370–1374.

Castagnola, E., Ansaldo, A., Maggiolini, E., Ius, T., Skrap, M., Ricci, D., and Fadiga, L. (2014). Smaller, softer, lower-impedance electrodes for human neuroprosthesis: a pragmatic approach. Front Neuroeng *7*, 8.

Chan, G., and Mooney, D.J. (2008). New materials for tissue engineering: towards greater control over the biological response. Trends Biotechnol. *26*, 382–392.

Chen, S., and Allen, M.G. (2012). Extracellular matrix-based materials for neural interfacing. MRS Bull. *37*, 606–613.

Chen, R.J., Bangsaruntip, S., Drouvalakis, K.A., Kam, N.W.S., Shim, M., Li, Y., Kim, W., Utz, P.J., and Dai, H. (2003). Noncovalent functionalization of carbon nanotubes for highly specific electronic biosensors. Proc. Natl. Acad. Sci. USA *100*, 4984–4989.

Chen, Z., Ren, W., Gao, L., Liu, B., Pei, S., and Cheng, H.-M. (2011). Three-dimensional flexible and conductive interconnected graphene networks grown by chemical vapour deposition. Nat. Mater. *10*, 424–428.

Chen, J.Y., Pei, W., Chen, S., Wu, X., Zhao, S., Wang, H., and Chen, H. (2013). Poly(3,4-ethylenedioxythiophene) (PEDOT) as interface material for improving electrochemical performance of microneedles array-based dry electrode. Sens. Actuators B Chem. *188*, 747–756.

Choi, W.M., Song, J., Khang, D.-Y., Jiang, H., Huang, Y.Y., and Rogers, J.A. (2007). Biaxially stretchable "wavy" silicon nanomembranes. Nano Lett. *7*, 1655–1663.

Chung, K., Wallace, J., Kim, S.-Y., Kalyanasundaram, S., Andalman, A.S., Davidson, T.J., Mirzabekov, J.J., Zalocusky, K.A., Mattis, J., Denisin, A.K., et al. (2013). Structural and molecular interrogation of intact biological systems. Nature *497*, 332–337.

Cogan, S.F. (2008). Neural stimulation and recording electrodes. Annu. Rev. Biomed. Eng. *10*, 275–309.

Collura, T.F. (1993). History and evolution of electroencephalographic instruments and techniques. J. Clin. Neurophysiol. *10*, 476–504.

Cui, Y., Wei, Q., Park, H., and Lieber, C.M. (2001). Nanowire nanosensors for highly sensitive and selective detection of biological and chemical species. Science *293*, 1289–1292.

Debener, S., Minow, F., Emkes, R., Gandras, K., and de Vos, M. (2012). How about taking a low-cost, small, and wireless EEG for a walk? Psychophysiology *49*, 1617–1621.

Deisseroth, K. (2011). Optogenetics. Nat. Methods *8*, 26–29.

Denk, W., and Svoboda, K. (1997). Photon upmanship: why multiphoton imaging is more than a gimmick. Neuron *18*, 351–357.

Edgington, R.J., Thalhammer, A., Welch, J.O., Bongrain, A., Bergonzo, P., Scorsone, E., Jackman, R.B., and Schoepfer, R. (2013). Patterned neuronal networks using nanodiamonds and the effect of varying nanodiamond properties on neuronal adhesion and outgrowth. J. Neural Eng. *10*, 056022.

Escabí, M.A., Read, H.L., Viventi, J., Kim, D.H., Higgins, N.C., Storace, D.A., Liu, A.S., Gifford, A.M., Burke, J.F., Campisi, M., et al. (2014). A high-density, high-channel count, multiplexed μECoG array for auditory-cortex recordings. J. Neurophysiol. *112*, 1566–1583.

Fan, J.A., Yeo, W.H., Su, Y., Hattori, Y., Lee, W., Jung, S.Y., Zhang, Y., Liu, Z., Cheng, H., Falgout, L., et al. (2014). Fractal design concepts for stretchable electronics. Nat. Commun. *5*, 3266.

Fiedler, P., Pedrosa, P., Griebel, S., Fonseca, C., Vaz, F., Zanow, F., and Haueisen, J. (2011). Novel flexible dry PU/TiN-multipin electrodes: first application in EEG measurements. Conf. Proc. IEEE Eng. Med. Biol. Soc. *2011*, 55–58.

Fine, A., Amos, W.B., Durbin, R.M., and McNaughton, P.A. (1988). Confocal microscopy: applications in neurobiology. Trends Neurosci. *11*, 346–351.

Flusberg, B.A., Nimmerjahn, A., Cocker, E.D., Mukamel, E.A., Barretto, R.P., Ko, T.H., Burns, L.D., Jung, J.C., and Schnitzer, M.J. (2008). High-speed, miniaturized fluorescence microscopy in freely moving mice. Nat. Methods *5*, 935–938.

George, P.M., Lyckman, A.W., LaVan, D.A., Hegde, A., Leung, Y., Avasare, R., Testa, C., Alexander, P.M., Langer, R., and Sur, M. (2005). Fabrication and biocompatibility of polypyrrole implants suitable for neural prosthetics. Biomaterials *26*, 3511–3519.

Gerard, M., Chaubey, A., and Malhotra, B.D. (2002). Application of conducting polymers to biosensors. Biosens. Bioelectron. *17*, 345–359.

Gerwig, R., Fuchsberger, K., Schroeppel, B., Link, G.S., Heusel, G., Kraushaar, U., Schuhmann, W., Stett, A., and Stelzle, M. (2012). PEDOT-CNT composite microelectrodes for recording and electrostimulation applications: fabrication, morphology, and electrical properties. Front Neuroeng *5*, 8.

Ghosh, K.K., Burns, L.D., Cocker, E.D., Nimmerjahn, A., Ziv, Y., Gamal, A.E., and Schnitzer, M.J. (2011). Miniaturized integration of a fluorescence microscope. Nat. Methods *8*, 871–878.

Green, R.A., Baek, S., Poole-Warren, L.A., and Martens, P.J. (2010). Conducting polymer-hydrogels for medical electrode applications. Sci. Technol. Adv. Mater. *11*, 014107.

Green, R.A., Lim, K.S., Henderson, W.C., Hassarati, R.T., Martens, P.J., Lovell, N.H., and Poole-Warren, L.A. (2013). Living electrodes: tissue engineering the neural interface. Proc. IEEE Eng. Med. Biol. Soc. Conf. 6957–6960.

Grill, W.M., Norman, S.E., and Bellamkonda, R.V. (2009). Implanted neural interfaces: biochallenges and engineered solutions. Annu. Rev. Biomed. Eng. *11*, 1–24.

Guimarda, N.K., Gomezb, N., and Schmidt, C.E. (2007). Conducting polymers in biomedical engineering. Prog. Polym. Sci. *32*, 876–921.

Guo, L., Ma, M., Zhang, N., Langer, R., and Anderson, D.G. (2014). Stretchable polymeric multielectrode array for conformal neural interfacing. Adv. Mater. *26*, 1427–1433.

HajjHassan, M., Chodavarapu, V., and Musallam, S. (2008). NeuroMEMS: Neural probel microtechnologies. Sensors (Basel Switzerland) *8*, 6704–6726.

He, W., and Bellamkonda, R. (2008). Indwelling Neural Implants: Strategies for Contending with the. In Vivo Environment, W.M. Reichert, ed. (Boca Raton, FL: CRC Press).

Hopper, A.P., Dugan, J.M., Gill, A.A., Fox, O.J.L., May, P.W., Haycock, J.W., and Claeyssens, F. (2014). Amine functionalized nanodiamond promotes cellular adhesion, proliferation and neurite outgrowth. Biomed. Mater. *9*, 045009.

Humpolicek, P., Kasparkova, V., Saha, P., and Stejskal, J. (2012). Biocompatibility of polyaniline. Synth. Met. *162*, 722–727.

Jacobs, C.B., Peairs, M.J., and Venton, B.J. (2010). Review: Carbon nanotube based electrochemical sensors for biomolecules. Anal. Chim. Acta *662*, 105–127.

Jang, K.I., Han, S.Y., Xu, S., Mathewson, K.E., Zhang, Y., Jeong, J.W., Kim, G.T., Webb, R.C., Lee, J.W., Dawidczyk, T.J., et al. (2014). Rugged and breathable forms of stretchable electronics with adherent composite substrates for transcutaneous monitoring. Nat. Commun. *5*, 4779.

Jung, H.C., Moon, J.H., Baek, D.H., Lee, J.H., Choi, Y.Y., Hong, J.S., and Lee, S.H. (2012). CNT/PDMS composite flexible dry electrodes for long-term ECG monitoring. IEEE Trans. Biomed. Eng. *59*, 1472–1479.

Kang, M., Jung, S., Zhang, H., Kang, T., Kang, H., Yoo, Y., Hong, J.-P., Ahn, J.-P., Kwak, J., Jeon, D., et al. (2014). Subcellular neural probes from single-crystal gold nanowires. ACS Nano *8*, 8182–8189.

Khodagholy, D., Doublet, T., Gurfinkel, M., Quilichini, P., Ismailova, E., Leleux, P., Herve, T., Sanaur, S., Bernard, C., and Malliaras, G.G. (2011). Highly conformable conducting polymer electrodes for in vivo recordings. Adv. Mater. *23*, H268–H272.

Kim, D.H., Viventi, J., Amsden, J.J., Xiao, J., Vigeland, L., Kim, Y.S., Blanco, J.A., Panilaitis, B., Frechette, E.S., Contreras, D., et al. (2010). Dissolvable films of silk fibroin for ultrathin conformal bio-integrated electronics. Nat. Mater. *9*, 511–517.

Kim, D.H., Lu, N., Ma, R., Kim, Y.S., Kim, R.H., Wang, S., Wu, J., Won, S.M., Tao, H., Islam, A., et al. (2011). Epidermal electronics. Science *333*, 838–843.

Kim, D.H., Ghaffari, R., Lu, N., and Rogers, J.A. (2012). Flexible and stretchable electronics for biointegrated devices. Annu. Rev. Biomed. Eng. *14*, 113–128.

Kim, T.I., McCall, J.G., Jung, Y.H., Huang, X., Siuda, E.R., Li, Y., Song, J., Song, Y.M., Pao, H.A., Kim, R.H., et al. (2013). Injectable, cellular-scale optoelectronics with applications for wireless optogenetics. Science *340*, 211–216.

Kozai, T.D.Y., Langhals, N.B., Patel, P.R., Deng, X., Zhang, H., Smith, K.L., Lahann, J., Kotov, N.A., and Kipke, D.R. (2012). Ultrasmall implantable composite microelectrodes with bioactive surfaces for chronic neural interfaces. Nat. Mater. *11*, 1065–1073.

Kuzum, D., Takano, H., Shim, E., Reed, J.C., Juul, H., Richardson, A.G., de Vries, J., Bink, H., Dichter, M.A., Lucas, T.H., et al. (2014). Transparent and flexible low noise graphene electrodes for simultaneous electrophysiology and neuroimaging. Nat. Commun. *5*, 5259.

Ledochowitsch, P., Olivero, E., Blanche, T., and Maharbiz, M.M. (2011). A transparent μECoG array for simultaneous recording and optogenetic stimulation. Proc. IEEE Eng. Med. Biol. Soc. Conf. 2937–2940.

Lee, P., Lee, J., Lee, H., Yeo, J., Hong, S., Nam, K.H., Lee, D., Lee, S.S., and Ko, S.H. (2012). Highly stretchable and highly conductive metal electrode by very long metal nanowire percolation network. Adv. Mater. *24*, 3326–3332.

Leleux, P., Badier, J.M., Rivnay, J., Bénar, C., Hervé, T., Chauvel, P., and Malliaras, G.G. (2014). Conducting polymer electrodes for electroencephalography. Adv Healthc Mater *3*, 490–493.

Li, N., Zhang, Q., Gao, S., Song, Q., Huang, R., Wang, L., Liu, L., Dai, J., Tang, M., and Cheng, G. (2013). Three-dimensional graphene foam as a biocompatible and conductive scaffold for neural stem cells. Sci Rep *3*, 1604.

Liu, X., Yue, Z., Higgins, M.J., and Wallace, G.G. (2011). Conducting polymers with immobilised fibrillar collagen for enhanced neural interfacing. Biomaterials *32*, 7309–7317.

Livet, J., Weissman, T.A., Kang, H., Draft, R.W., Lu, J., Bennis, R.A., Sanes, J.R., and Lichtman, J.W. (2007). Transgenic strategies for combinatorial expression of fluorescent proteins in the nervous system. Nature *450*, 56–62.

Logothetis, N.K. (2008). What we can do and what we cannot do with fMRI. Nature *453*, 869–878.

Lu, Y., Wang, D., Li, T., Zhao, X., Cao, Y., Yang, H., and Duan, Y.Y. (2009). Poly(vinyl alcohol)/poly(acrylic acid) hydrogel coatings for improving electrode-neural tissue interface. Biomaterials *30*, 4143–4151.

Merrill, D.R., Bikson, M., and Jefferys, J.G. (2005). Electrical stimulation of excitable tissue: design of efficacious and safe protocols. J. Neurosci. Methods *141*, 171–198.

Minev, I.R., Chew, D.J., Delivopoulos, E., Fawcett, J.W., and Lacour, S.P. (2012). High sensitivity recording of afferent nerve activity using ultracompliant microchannel electrodes: an acute in vivo validation. J. Neural Eng. *9*, 026005.

Minev, I.R., Musienko, P., Hirsch, A., Barraud, Q., Wenger, N., Moraud, E.M., Gandar, J., Capogrosso, M., Milekovic, T., Asboth, L., et al. (2015). Electronic dura mater for long-term multimodal neural interfaces. Science *347*, 159–163.

Mozota, J., and Conway, B.E. (1983). Surface and bulk processes at oxidized iridium electrodes—I. Monolayer stage and transition to reversible multilayer oxide film behaviour. Electrochim. Acta *28*, 1–8.

Niedermayer, E., and Lopes Da Silva, F.H. (2005). Electroencephalography: Basic Principles, Clinical Applications, and Related Fields, Fifth Edition. (Philadelphia, PA: Lippincott Williams & Wilkins).

Ozden, I., Wang, J., Lu, Y., May, T., Lee, J., Goo, W., O'Shea, D.J., Kalanithi, P., Diester, I., Diagne, M., et al. (2013). A coaxial optrode as multifunction write-read probe for optogenetic studies in non-human primates. J. Neurosci. Methods *219*, 142–154.

Pan, L., Yu, G., Zhai, D., Lee, H.R., Zhao, W., Liu, N., Wang, H., Tee, B.C.-K., Shi, Y., Cui, Y., and Bao, Z. (2012). Hierarchical nanostructured conducting polymer hydrogel with high electrochemical activity. Proc. Natl. Acad. Sci. USA *109*, 9287–9292.

Park, M., Im, J., Shin, M., Min, Y., Park, J., Cho, H., Park, S., Shim, M.-B., Jeon, S., Chung, D.-Y., et al. (2012). Highly stretchable electric circuits from a composite material of silver nanoparticles and elastomeric fibres. Nat. Nanotechnol. *7*, 803–809.

Patolsky, F., and Lieber, C.M. (2005). Nanowire nanosensors. Mater. Today *8*, 20–28.

Petrossians, A., Whalen Iii, J.J., Weiland, J.D., and Mansfeld, F. (2011). Electrodeposition and characterization of thin-film platinum-iridium alloys for biological interfaces. J. Electrochem. Soc. *158*, D269–D276.

Phelps, M.E. (2000). PET: the merging of biology and imaging into molecular imaging. J. Nucl. Med. *41*, 661–681.

Polikov, V.S., Tresco, P.A., and Reichert, W.M. (2005). Response of brain tissue to chronically implanted neural electrodes. J. Neurosci. Methods *148*, 1–18.

Rao, L., Zhou, H., Li, T., Li, C., and Duan, Y.Y. (2012). Polyethylene glycol-containing polyurethane hydrogel coatings for improving the biocompatibility of neural electrodes. Acta Biomater. *8*, 2233–2242.

Rogers, J.A., Someya, T., and Huang, Y. (2010). Materials and mechanics for stretchable electronics. Science *327*, 1603–1607.

Rubehn, B., Wolff, S.B.E., Tovote, P., Lüthi, A., and Stieglitz, T. (2013). A polymer-based neural microimplant for optogenetic applications: design and first in vivo study. Lab Chip *13*, 579–588.

Seo, D., Carmena, J.M., Rabaey, J.M., Maharbiz, M.M., and Alon, E. (2014). Model validation of untethered, ultrasonic neural dust motes for cortical recording. J. Neurosci. Methods. http://dx.doi.org/10.1016/j.jneumeth.2014.07.025.

Tian, B., Cohen-Karni, T., Qing, Q., Duan, X., Xie, P., and Lieber, C.M. (2010). Three-dimensional, flexible nanoscale field-effect transistors as localized bioprobes. Science *329*, 830–834.

Tian, B., Liu, J., Dvir, T., Jin, L., Tsui, J.H., Qing, Q., Suo, Z., Langer, R., Kohane, D.S., and Lieber, C.M. (2012). Macroporous nanowire nanoelectronic scaffolds for synthetic tissues. Nat. Mater. *11*, 986–994.

Tien, L.W., Wu, F., Tang-Schomer, M.D., Yoon, E., Omenetto, F.G., and Kaplan, D.L. (2014). Silk as a multifunctional biomaterial substrate for reduced glial scarring around brain-penetrating electrodes. Adv. Funct. Mater. *23*, 3185–3193.

Tsang, W.M., Stone, A.L., Otten, D., Aldworth, Z.N., Daniel, T.L., Hildebrand, J.G., Levine, R.B., and Voldman, J. (2012). Insect-machine interface: a carbon nanotube-enhanced flexible neural probe. J. Neurosci. Methods *204*, 355–365.

Viventi, J., Kim, D.H., Moss, J.D., Kim, Y.S., Blanco, J.A., Annetta, N., Hicks, A., Xiao, J., Huang, Y., Callans, D.J., et al. (2010). A conformal, bio-Interfaced class of silicon electronics for mapping cardiac electrophysiology. Sci. Transl. Med. *2*, 24ra2.

Viventi, J., Kim, D.H., Vigeland, L., Frechette, E.S., Blanco, J.A., Kim, Y.S., Avrin, A.E., Tiruvadi, V.R., Hwang, S.W., Vanleer, A.C., et al. (2011). Flexible, foldable, actively multiplexed, high-density electrode array for mapping brain activity in vivo. Nat. Neurosci. *14*, 1599–1605.

Wang, J. (2005). Carbon-nanotube based electrochemical biosensors: A review. Electroanalysis *17*, 7–14.

Wang, Y., Li, Z., Wang, J., Li, J., and Lin, Y. (2011). Graphene and graphene oxide: biofunctionalization and applications in biotechnology. Trends Biotechnol. *29*, 205–212.

Ward, M.P., Rajdev, P., Ellison, C., and Irazoqui, P.P. (2009). Toward a comparison of microelectrodes for acute and chronic recordings. Brain Res. *1282*, 183–200.

Ware, T., Simon, D., Liu, C., Musa, T., Vasudevan, S., Sloan, A., Keefer, E.W., Rennaker, R.L., 2nd, and Voit, W. (2014). Thiol-ene/acrylate substrates for softening intracortical electrodes. J. Biomed. Mater. Res. B Appl. Biomater. *102*, 1–11.

Wise, K.D., Sodagar, A.M., Yao, Y., Gulari, M.N., and Najafi, K. (2008). Microelectrodes, microelectronics, and implantable neural microsystems. Proc. IEEE *96*, 1184–1202.

Wolpaw, J.R., and McFarland, D.J. (2004). Control of a two-dimensional movement signal by a noninvasive brain-computer interface in humans. Proc. Natl. Acad. Sci. USA *101*, 17849–17854.

Wu, F., Im, M., and Yoon, E. (2011). A flexible fish-bone-shaped neural probe strengthened by biodegradable silk coating for enhanced biocompatibility. Proc. Transducers. 966–969.

Wu, F., Lee, T., Chen, F., Kaplan, D., Berke, J., and Yoon, E. (2013a). A multishank silk-backed parylene neural probe for reliable chronic recording. Proc. Transducers. 888–891.

Wu, F., Stark, E., Im, M., Cho, I.J., Yoon, E.S., Buzsáki, G., Wise, K.D., and Yoon, E. (2013b). An implantable neural probe with monolithically integrated dielectric waveguide and recording electrodes for optogenetics applications. J. Neural Eng. *10*, 056012.

Xiang, Z., Yen, S.-C., Xue, N., Sun, T., Tsang, W.M., Zhang, S., Liao, L.-D., Thakor, N.V., and Lee, C. (2014). Ultra-thin flexible polyimide neural probe embedded in a dissolvable maltose-coated microneedle. J. Micromech. Microeng. *24*, 065015.

Xu, S., Zhang, Y., Jia, L., Mathewson, K.E., Jang, K.I., Kim, J., Fu, H., Huang, X., Chava, P., Wang, R., et al. (2014). Soft microfluidic assemblies of sensors, circuits, and radios for the skin. Science *344*, 70–74.

Yeo, W.H., Kim, Y.S., Lee, J., Ameen, A., Shi, L., Li, M., Wang, S., Ma, R., Jin, S.H., Kang, Z., et al. (2013). Multifunctional epidermal electronics printed directly onto the skin. Adv. Mater. *25*, 2773–2778.

Zang, J., Ryu, S., Pugno, N., Wang, Q., Tu, Q., Buehler, M.J., and Zhao, X. (2013). Multifunctionality and control of the crumpling and unfolding of large-area graphene. Nat. Mater. *12*, 321–325.

Zhang, S., Tsang, W.M., Srinivas, M., Sun, T., Singh, N., Kwong, D.-L., and Lee, C. (2014). Development of silicon electrode enhanced by carbon nanotube and gold nanoparticle composites on silicon neural probe fabricated with complementary metal-oxide-semiconductor process. Appl. Phys. Lett. *104*, 193105.

Zheng, G., Patolsky, F., Cui, Y., Wang, W.U., and Lieber, C.M. (2005). Multiplexed electrical detection of cancer markers with nanowire sensor arrays. Nat. Biotechnol. *23*, 1294–1301.